Phase retrieval for arbitrary complex-valued objects using structured illumination

A.V. Kuzmenko[1], and O.M. Butok[2]

[1]Branch of Applied Optics, Institute of Physics of National Academy of Sciences of Ukraine, Kyiv, Ukraine
[2]Institute for Information Recording of National Academy of Sciences of Ukraine, Kyiv, Ukraine
avkuz@iop.kiev.ua

One of the most difficult inverse diffraction problems is the so-called, ill-posed, problem of retrieving a complex-valued object $f(r)$, $r = (x; y)$, from the amplitude distribution pattern $g_0(r_S)$ of the complex-valued field $g(r_S)$, $r_S = (x_S; y_S)$, in the Fresnel or Fraunhofer diffraction zone, which plays a very significant role in those domains of science and technology where coherent radiation and its registration are deal with [1], and in short form is written as

$$\text{find } f \text{ such that } \langle G; f \rangle = g_0; \tag{1}$$

where $f \in C^{N \times N}$ is the sought complex-valued object function, $G \in C^{M \times N}$ is the Fresnel or Fourier transform operator, and $g_0 \in R_+^{M \times M}$ is the amplitude measured in the diffraction plane. In Eq. (1) the angle brackets mean the scalar product.

In our work, a new method of the solution of non-convex CDI problem (1) using structured illumination and alternating projection (AP) algorithms is proposed.

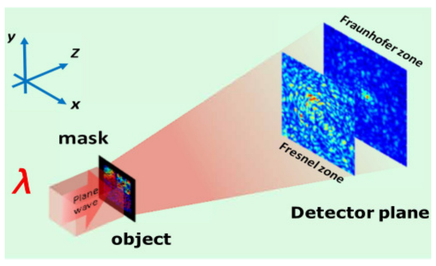

Figure 1: A typical scheme for structured illuminations in diffraction imaging using a mask: the plane coherent wave ( ) illuminates the mask + sample pair, encoded diffraction pattern is measured by a detector in Fresnel or Fraunhofer plane.

A. Method solution

Let us consider the following method of phase retrieval using the optical scheme shown in Fig. 1. For structuring the illuminating field, two random binary amplitude masks, direct having transmittance $\Delta_1(r)$ and its inverse with transmittance $\Delta_2(r)$ ones, are applied (i.e. the masks in the pair are complementary to each other). For simplicity, let us assume that the masks are superimposed immediately onto the object, i.e., the masked object can be represented as $f_\Delta(r) = \Delta(r) f(r)$ (the notation Δ will be used for both masks). The intensity of the diffracted field registered in the Fresnel or Fraunhofer plane also makes it possible to determine two amplitude sets $g_0^1(r_S)$ and $g_0^2(r_S)$ needed to retrieve the object wave field. The retrieval algorithm is applied separately to each of the available pairs, $\langle \Delta_1(r); g_0^1(r_S) \rangle$ and $\langle \Delta_2(r); g_0^2(r_S) \rangle$. Hence, the original problem is split into two subtasks of the same type, which can be solved on a computer in parallel.

The field retrieval takes place on transparent pixels of each mask. Since the transparent pixels in the direct and reverse masks cover together the entire area of the object, the sum of the complex amplitudes $f_{\Delta 1}(r)$ and $f_{\Delta 2}(r)$ retrieved at the transparent areas of the masks give us the general solution of the problem,

$$f_{rec}(r) = f_{\Delta 1}(r) + f_{\Delta 2}(r); \tag{2}$$

with an accuracy to the global phase. The phase components of the obtained solutions $f_{\Delta 1}(r)$ and $f_{\Delta 2}(r)$ are usually shifted with respect to each other by an arbitrary phase constant and, hence, have to be matched. The solutions can be easily brought into agreement with each other provided that the direct and reverse masks contain a small number of overlapping transparent pixels. The phase values at those pixels are used to eliminate the phase shift between the solutions.

B. Numerical simulation results

To test the efficiency of the proposed method, model experiments, namely, the solution of the CDI problem for objects of various types (some of them are shown in Fig. 2), were performed.

For the cases of Fresnel and Fraunhofer diffraction, algorithms have been developed where the Fast Fourier Transform is applied. In particular, in the algorithm for calculating the paraxial Fresnel diffraction, the sampling intervals in the object and diffraction planes satisfied the known relationship

$$N \Delta x_0 \Delta x_Z = \lambda Z; \tag{3}$$

where Δx_0 and Δx_Z are the sampling intervals (the pixel sizes) in the object and diffraction planes, respectively; N is the number of counts along the axes $(x; y)$ and $(x_S; y_S)$, respectively, in those planes; Z is the distance between the object and diffraction planes; and λ is the radiation wavelength. Formula (3) provides a rather high calculation accuracy for Z-values lying in the "middle" Fresnel diffraction zone.

Two coded diffraction patterns (CDPs) and the corresponding $g_0^1(r_S)$ and $g_0^2(r_S)$ in the Fresnel or Fraunhofer diffraction planes were obtained, first, by masking the object. Afterward, in this form or with the addition of noise of various types, they were used as initial data for calculations. For each of the $\langle \Delta_1(r); g_0^1(r_S) \rangle$ and $\langle \Delta_2(r); g_0^2(r_S) \rangle$ pairs, separately, an iterative calculation was carried out using modified ER and HIO algorithms presented, respectively, as

$$f^{(n+1)}(r) = \begin{cases} P_S \Delta(r) f^{(n)}(r) & \text{if } r \in S; \\ 0 & \text{otherwise,} \end{cases} \tag{4}$$

and

$$f^{(n+1)}(r) = \begin{cases} P_S \Delta(r) f^{(n)}(r) & \text{if } r \in S; \\ (I - \beta P_S) \Delta(r) f^{(n)}(r) & \text{otherwise,} \end{cases} \tag{5}$$

where S is the object's support, $P_S = F^{-1} R_S F^{+1}$, F^{-1} is the direct (+1) or inverse (1) Fresnel (Fourier) transform, R_S is the operation that substitutes the amplitude $g_{(n)}(r_S)$ obtained after the n-th iteration by $g_0(r_S)$, the T_S operator before the R_S operator makes the phase of the function $g_{(n)}(r_S) = |g_{(n)}(r_S)| \exp(i \varphi_{(n)}(r_S))$ equal to zero at those points where the modulus of the function is close to zero (in general, the application T_S is not strictly necessary, but in some cases it can speed up the convergence of the algorithm), I is the identity operator, and β is the HIO algorithm parameter. A specific feature of the presented ER and HIO algorithms, which should be emphasized, is the availability of the operation consisting in the masking of the reconstructed field at each iteration step. Mathematically, this operation is represented by the product of the field function $f^{(n)}(r)$ and the mask transmission function $\Delta(r)$.

In the simplest case, the initial estimate of the sought function $f_\Delta(r)$ can be chosen in the form of a plane wave, $f^{(0)}(r) = \exp(i \varphi_0)$, where φ_0 is an arbitrary phase constant. When using the ER-HIO-ER calculation scheme, the ratio between the numbers of ER and HIO iterations could be controlled; the constant β was selected from the interval $(0{:}2; 0{:}9)$. In the course of iterations, the accuracy of the obtained solution was monitored in two ways: as

$$E^{(n)} = \frac{\sum_{r \notin S} |f^{(n)}|^2}{\sum_{r \in S} |f^{(n)}|^2} \tag{6}$$

in the object plane and as the mean-square deviation of the amplitude $g_{(n)}(r_S)$ from $g_0(r_S)$ in the diffraction plane.

As was already indicated, the general solution is obtained as the sum of the solutions found separately for each of the masks $\Delta_1(r)$ and $\Delta_2(r)$ [see Eq. (2)]. The calculations were carried out for the oversampling ratio $\alpha \geq 2$, where

$$\alpha = \frac{\text{total Fourier (Fresnel) magnitude data number}}{\text{total unknown-valued object pixel number}}. \tag{7}$$

Such a definition for α seems to have been first used when solving the CDI problem in the case of Fourier diffraction, although, strictly speaking, the oversampling ratio should be defined as the ratio α_s = [Fourier amplitude data number]=[unknown-valued object pixel number] along *each* coordinate axis. But as was shown in, in some peculiar formulations of the phase problem, correct solutions can be obtained under less strict requirements to the oversampling ratio, which are reflected in formula (7). The results of numerical simulation show that the parameter α defined via formula (7) successfully works when solving the phase problem for a complex-valued object not only in the case of Fraunhofer diffraction, but also in the case of Fresnel one. Nevertheless, it is obvious that the application of definition (7) has to be theoretically justified in the general case of Fresnel diffraction.

Since the perfect objects $f(r)$ are known to us during modeling (the initial data $g_0^1(r_S)$ and $g_0^2(r_S)$ were obtained from them), then, among other characteristics, we can determine the signal-to-noise ratio (SNR) in the resulting image $f_{rec}(r)$,

$$SNR(n) = \frac{\sum_r |f_{rec}^{(n)}(r)|^2}{\sum_r |f(r)| - c_0 f_{rec}^{(n)}(r)|^2}; \tag{8}$$

where c_0 is the scaling factor.

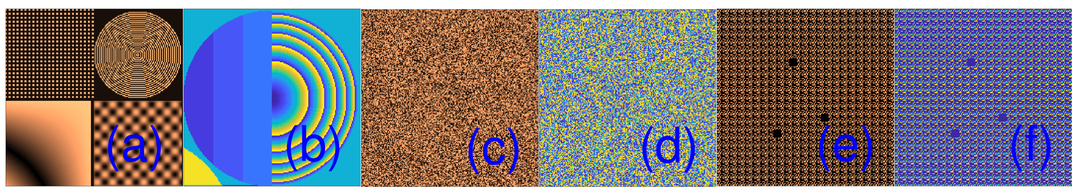

Figure 2: Complex-valued 181 181 test-objects with: 1. Deterministic amplitude (a) and phase (b); 2. Random amplitude (c) and phase (d); 3. Crystal-like with defects and the random distribution of amplitudes (e) and phases (f) in cells of the structure. The size of one cell is 8 8 pixels.

The retrieval problem was solved by us for the cases of both Fresnel and Fraunhofer diffraction, for each object presented in Fig. 2, for $\lambda = 0{:}6328$ m and the oversampling ratios $\alpha = 4$, 3, and 2. The indicated values of α were provided by supplementing the object with zeros to the required format. The parameters for Fresnel diffraction were $x_0 = 64$ m and $Z = 1{:}6570$ m. The value of x_Z is determined from relationship (3).

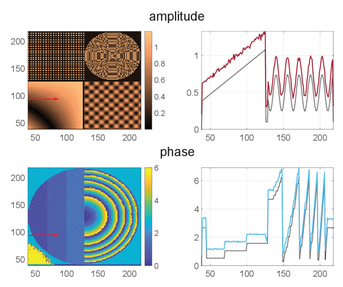

Figure 3: Complex-valued field recovery corresponding to the data in Table 1, section ER/HIO/ER for Fresnel diffraction. Panels (a), (b), and (c) correspond to objects 1, 2, and 3. Panels (b) and (c) to increase the resolution contain only image fragments and their cross sections. The place and direction of sections of D2 - representations are indicated by arrows. Comparison of the ideal (dotted lines) and vertically shifted reconstructed (solid lines) curves demonstrates a fairly high recovery accuracy.

Figure 4: Convergence performance of algorithm on the noise type and its level in the original data $g_0(r_S)$ for (a) - object 2, (b) - object 3. Fresnel diffraction, recovery by ER/HIO/ER = 40/120/40 iterations at $\beta = 0{:}6$.

The results of model experiments on the reconstruction of the object field for both cases of diffraction, using modified ER and HIO algorithms (4) and (5), are presented in [1], as well as in Figs. 3 and 4. The amplitude distributions g_0^1 and g_0^2 representing CDPs in the Fresnel and Fraunhofer diffraction zones were taken in the calculations both ideal and containing "registration" noise. In the latter case, the generated additive noise of Poisson, Gauss or Exponential type of a given level was added to the ideal g_0 distribution. The recovery accuracy depending on the number of iterations (ITR) was monitored using relation for average retrieval error $E(n) = \frac{1}{2}\left(E_1^{(n)} + E_2^{(n)}\right)$ (see (6)) and the ratio (8) for SNR. In the absence of noise, an almost exact restoration of the amplitude-phase distribution of all three objects was obtained (see, for example, the convergence results at zero noise for objects 2 and 3 in Figure 4). Table I in [1] presents the results of solving the CDI - problem in the case of noisy initial data g_0. As we can see, in the case of Fraunhofer diffraction, to achieve a reconstruction accuracy comparable to the Fresnel one, 1.5 - 2 times more iterations of both ER or ER/HIO/ER algorithms are required. Approximately the same story is observed with the ratio of the amounts of ER iterations and total ER/HIO/ER iterations to each other. On Figure 3 shows the results of complex-valued field reconstruction modeling, illustrating the convergence data given in Table I in [1], namely the ER/HIO/ER section for Fresnel diffraction. The influence of the type of probabilistic distribution of noise and its level in the initial data on the convergence of the algorithm is shown in Figure 4. As can be seen, the noise type, in contrast to the noise level, does not substantially affect the convergence of the algorithm. The properties of the reconstructed fields in the case of Fraunhofer diffraction did not differ in any way from the properties obtained for Fresnel one and, therefore, are not discussed.

Conclusion

The method presented in this paper demonstrates how the CDI problem can be successfully solved for arbitrary complex-valued support-constrained objects making use of two diffraction patterns (they are obtained with the help of two random binary amplitude masks applied to structure the illuminating field) and modified ER and HIO algorithms. The successful noise-resistant retrieval of images of various complex-valued objects with an accuracy to the global phase was obtained for the oversampling ratios $\alpha \geq 2$ in particular, $\alpha = 4$; 3, and $2 \leq \alpha$ and using a relatively small number of iterations. The influence of the degree of noisiness of the initial data by noises of various types on the process of restoring objects is also studied.

The proposed method and the results obtained can be compared with the solution methods and experimental results presented in the patent [2], which, like ours, is devoted to the issue of minimizing the number of masks needed to solve the CDI problem.

In conclusion, due both to the use of structured illumination and to the performance of the modified ER and HIO algorithms, our method may be used to recovery a complex object in a simple and effective way for coherent radiation of any type, up to X-rays.

References

[1] A.V. Kuzmenko, and O. M. Butok, "Phase retrieval for arbitrary complex-valued objects using structured illumination," Preprints Optica Open.

[2] US patent #11,237,059 B1 by Ersoy (2022).